THE JOURNAL OF BIOLOGICAL CHEMISTRY
Vol. 280, No. 6, Issue of February 11, pp. 4254–4263, 2005
Printed in U.S.A.

Mitochondrial $O_2^{\cdot-}$ and H_2O_2 Mediate Glucose Deprivation-induced Cytotoxicity and Oxidative Stress in Human Cancer Cells*

Received for publication, October 13, 2004
Published, JBC Papers in Press, November 23, 2004, DOI 10.1074/jbc.M411662200

Iman M. Ahmad‡, Nukhet Aykin-Burns‡, Julia E. Sim§, Susan A. Walsh‡, Ryuji Higashikubo§, Garry R. Buettner‡, Sujatha Venkataraman‡, Michael A. Mackey¶‖, Shawn W. Flanagan‡, Larry W. Oberley‡, and Douglas R. Spitz‡§**

From the ‡Free Radical and Radiation Biology Program, Department of Radiation Oncology, Holden Comprehensive Cancer Center, The University of Iowa, Iowa City, Iowa 52242, the §Division of Radiation and Cancer Biology, Department of Radiation Oncology, Washington University, St. Louis, Missouri 63108, and the Departments of ¶Biomedical Engineering and ‖Radiology, The University of Iowa, Iowa City, Iowa 52242

The hypothesis that glucose deprivation-induced cytotoxicity in transformed human cells is mediated by mitochondrial $O_2^{\cdot-}$ and H_2O_2 was first tested by exposing glucose-deprived SV40-transformed human fibroblasts (GM00637G) to electron transport chain blockers (ETCBs) known to increase mitochondrial $O_2^{\cdot-}$ and H_2O_2 production (antimycin A (AntA), myxothiazol (Myx), or rotenone (Rot)). Glucose deprivation (2–8 h) in the presence of ETCBs enhanced parameters indicative of oxidative stress (*i.e.* GSSG and steady-state levels of oxygen-centered radicals) as well as cytotoxicity. Glucose deprivation in the presence of AntA also significantly enhanced cytotoxicity and parameters indicative of oxidative stress in several different human cancer cell lines (PC-3, DU145, MDA-MB231, and HT-29). In addition, human osteosarcoma cells lacking functional mitochondrial electron transport chains (rho(0)) were resistant to glucose deprivation-induced cytotoxicity and oxidative stress in the presence of AntA. In the absence of ETCBs, aminotriazole-mediated inactivation of catalase in PC-3 cells demonstrated increases in intracellular steady-state levels of H_2O_2 during glucose deprivation. Finally, in the absence of ETCBs, overexpression of manganese containing superoxide dismutase and/or mitochondrial targeted catalase using adenoviral vectors significantly protected PC-3 cells from toxicity and oxidative stress induced by glucose deprivation with expression of both enzymes providing greater protection than was seen with either alone. Overall, these findings strongly support the hypothesis that mitochondrial $O_2^{\cdot-}$ and H_2O_2 significantly contribute to glucose deprivation-induced cytotoxicity and metabolic oxidative stress in human cancer cells.

Oxidative stress results when the balance between steady-state levels of intracellular prooxidants exceeds cellular antioxidant capacity. Many cancer cells have low levels of several antioxidant enzymes (*i.e.* Mn-SOD[1] and catalase) (1, 2). It has also been suggested that cancer cells may exhibit defects in their mitochondrial electron transport chains that could lead to increased steady-state levels of prooxidants (*i.e.* superoxide and hydroperoxides) resulting from one-electron reduction of O_2 leading to a condition of metabolic oxidative stress (3). Most cancer cells maintain a high glycolytic rate; a phenomenon first described over 70 years ago and known as the Warburg effect (4). In addition to its role in energy production, glucose metabolism also leads to the formation of pyruvate and NADPH, both of which are believed to function in the cellular detoxification of hydroperoxides (5, 6). Pyruvate reacts directly with hydrogen peroxide and organic hydroperoxides (H_2O_2 and ROOH, respectively), resulting in the deacetylation of pyruvate to acetic acid and reduction of the peroxides to H_2O or ROH (5). NADPH provides electrons for the reduction of glutathione disulfide and oxidized thioredoxin, which is required for the efficient detoxification of H_2O_2 and ROOH by glutathione peroxidases and peroxiredoxins (3, 6–8). Given these observations it is logical to hypothesize that cancer cells might increase glucose metabolism as a compensatory mechanism to protect against intracellular hydroperoxides generated from mitochondrial electron transport chain activity. Several studies have demonstrated glucose deprivation-induced cytotoxicity and oxidative stress in cancer cells, but the role of mitochondrial $O_2^{\cdot-}$ and H_2O_2 in this phenomenon has not been clearly demonstrated (3, 7–8). We hypothesize that glucose deprivation in human cancer cells will result in a compromised ability to detoxify H_2O_2 derived from mitochondrial metabolism resulting in steady-state increases in hydroperoxides that contribute to glucose deprivation-induced cytotoxicity and oxidative stress.

To test the hypothesis that mitochondrial $O_2^{\cdot-}$ and H_2O_2 mediate glucose deprivation-induced oxidative stress and cytotoxicity in human cancer cells, three different approaches were utilized. First, the effect of ETCBs (known to increase $O_2^{\cdot-}$ and H_2O_2 production in isolated mitochondria) was determined in intact cells during glucose deprivation. Antimycin A was tested as a blocker of Complex III, myxothiazol was tested as a blocker of entry into Complex III, and rotenone was tested as a Complex I blocker (see Fig. 12). Second, rho(0) human cancer cells,

* This work was supported in part by National Institutes of Health Grants R01CA100045 and R01HL51469 (to D. R. S.), P01CA66081 (to G. R. B., S. V., L. W. O.), P01CA75556 (to R. H.), P20CA91709 (to I. M. A.), and R33CA94801 (to M. A. M.). The costs of publication of this article were defrayed in part by the payment of page charges. This article must therefore be hereby marked "*advertisement*" in accordance with 18 U.S.C. Section 1734 solely to indicate this fact.

** To whom correspondence should be addressed: B180 Medical Laboratories, Free Radical and Radiation Biology Program, The University of Iowa, IA City, IA 52242. Tel.: 319-335-8001; Fax: 319-335-8039; E-mail: douglas-spitz@uiowa.edu.

[1] The abbreviations used are: SOD, superoxide dismutase; ETCB, electron transport chain blocker; Mn-SOD, manganese superoxide dismutase; CuZn-SOD, copper-zinc superoxide dismutase; AntA, antimycin A; Myx, myxothiazol; Rot, rotenone; DNP, dinitrophenol; AT, 3-amino-1,2,4-triazole; Me_2SO, dimethyl sulfoxide; PBS, phosphate-buffered saline; GPx, glutathione peroxidase; MFI, mean fluorescence intensity; DMEM, Dulbecco's modified Eagle's medium; CMV, cytomegalovirus; DMPO, 5,5-dimethyl-1-pyrroline-*N*-oxide.

deficient in functional mitochondrial electron transport chains, were utilized. Finally, adenovirus-mediated transduction of mitochondrially targeted catalase (MitCat) or Mn-SOD was utilized to overexpress enzymatic scavengers of H_2O_2 and O_2^-, respectively, in human tumor cells prior to glucose deprivation in the absence of ETCBs.

The results of these experiments demonstrated that ETCBs dramatically enhanced glucose deprivation-induced cytotoxicity and parameters indicative of oxidative stress in all human tumor cell lines tested. Furthermore, rho(0) cells were resistant to increases in cytotoxicity and parameters indicative of oxidative stress during treatment with glucose deprivation in the presence of ETCBs. Finally, steady-state levels of reactive oxygen species (particularly H_2O_2) were increased during glucose deprivation in the presence and absence of ETCBs and overexpression of MitCat and Mn-SOD protected PC-3 cells from glucose deprivation-induced cytotoxicity and parameters indicative of oxidative stress in the absence of ETCBs. These results provide strong support for the hypothesis that mitochondria represent a primary source of O_2^- and H_2O_2 that significantly contributes to glucose deprivation-induced cytotoxicity and oxidative stress in human cancer cells.

EXPERIMENTAL PROCEDURES

Cells and Culture Conditions—GM00637G SV40 transformed human fibroblasts were obtained and cultured as described (3). HT-29 human colon carcinoma cells were obtained from ATCC and maintained in McCoy's 5A media supplemented with 10% fetal bovine serum. PC-3 human prostate cancer cells were obtained from ATCC, and maintained in F-12 media supplemented with 10% fetal bovine serum. DU145 and MDA-MB231 human prostate and breast cancer cells, respectively, were a gift from Dr. Mary Hendrix, University of Iowa, and maintained in RPMI media supplemented with 10% fetal bovine serum (9). Dr. Michael King (Thomas Jefferson University, Philadelphia, PA) kindly provided the human osteosarcoma 143BTK− rho(+) and rho(0) cells (10). These cells were grown in DMEM, 4.5 g/liter glucose supplemented with 5% fetal bovine serum and 50 μg/ml uridine for the rho(0) cells. All stock cultures were maintained in 5% CO_2 and air in a humidified 37 °C incubator in the absence of antibiotics. All cells were routinely tested for mycoplasma and found to be negative.

Glucose Deprivation Conditions and Cell Survival Experiments—Cells were plated in 60-mm tissue culture dishes and grown for 3 days in the presence of antibiotics (gentamycin). At the beginning of each experiment, the cells were rinsed with phosphate-buffered saline (PBS) to remove glucose and placed in glucose-free DMEM or RPMI 1640 media supplemented with 10% dialyzed serum as described previously (7, 8). Control cultures were treated identically except glucose was added back at the normal concentration found in the media. Then, drug treatment was initiated as appropriate. Cells were then placed in an incubator and at each time point, cells were trypsinized, counted, diluted, and plated for clonogenic cell survival assay as described previously (11). Surviving colonies were fixed and stained after 14 days and counted under a dissecting microscope.

Drug Treatment—AntA, Myx, Rot, dinitrophenol (DNP), and 3-amino-1,2,4-triazole (AT) were obtained from Sigma and used without further purification. Drugs were added to cells at final concentrations of 10 μM AntA and Myx, 50 μM Rot, 2 μM DNP, and 50 mM AT. Stock solutions of 10 mM AntA and Myx, 50 mM rotenone, and 2 mM DNP were dissolved in Me_2SO, whereas 5 M AT was dissolved in PBS, and the required volume was added directly to the cells to achieve the desired final concentrations. All cells were incubated in glucose-free medium containing dialyzed serum with different drugs for the specified times.

Measurement of Glutathione Levels—Following treatment, cells were scrape-harvested in PBS at 4 °C, centrifuged, the PBS discarded, and the cell pellets frozen at −80 °C. Samples were thawed and whole homogenates were prepared as described (7, 8). Total glutathione (GSH + GSSG) and glutathione disulfide (GSSG) were determined using a spectrophotometeric recycling assay (7, 8). All biochemical determinations were normalized to protein content using the method of Lowry *et al.* (12).

EPR Spin Trapping of Oxygen Centered Radicals—DMPO was purchased from Sigma (D-5766). The stock solution of DMPO was prepared with nanopure water. The solution was purified by multiple centrifugations through activated charcoal (Sigma, C-5385) and filtered. The concentration of DMPO was determined with a HP 8453 UV-visible spectrometer at $\epsilon_{227} = 7800\ M^{-1}\ cm^{-1}$. Purity was confirmed using EPR. EPR spectra were obtained using a Bruker X-band EMX spectrometer at room temperature. Instrument settings were: 9.77 GHz, microwave frequency; 100 kHz, modulation frequency; 40 milliwatt, nominal microwave power (13); 1.0 G, modulation amplitude; 3480 G center field for DMPO/$^{\cdot}$OH; 80 G/84 s scan rate; and 164-ms time constant. Each sample for EPR contained 7×10^6 freshly trypsinized cells in PBS and each spectrum was signal averaged, $n = 15$, to increase the signal-to-noise ratio.

Transduction of Antioxidant Enzymes—Replication incompetent adenoviral vectors, AdCMV BglII (AdBglII), AdCMV catalase (AdCAT), AdCMV mitochondrial catalase (AdMitCat), and AdCMV Mn-SOD (AdMn-SOD) were manufactured at The University of Iowa Gene Transfer Vector Core by inserting the gene of interest into the E1 region of an Ad5 E1/particle E3 deleted replication-deficient adenoviral vector. The cDNAs were all under the control of a CMV promotor. Except for AdMitCat, the adenovirus constructs were originally prepared by John Engelhardt, University of Iowa (14). The full-length catalase cDNA with the Mn-SOD mitochondrial leader sequence added to the construct were originally prepared by Dr. Andre Melendez (15). Cells were seeded until attached (overnight), and then the desired amount of viral particles was added with 1.8 ml of complete media per 60-mm dish for 24 h, then the media was changed and replaced by 4 ml of complete media and left for another 24 h prior to each experiment.

Catalase Activity Assay—Catalase activity was determined on whole homogenates by measuring the disappearance of 10 mM hydrogen peroxide ($\Delta\epsilon_{240} = 39.4\ M^{-1}\ cm^{-1}$) in 50 mM potassium phosphate, pH 7.0, monitored at 240 nm and the units were expressed as milli-*k* units/mg of protein as described (16).

Mn-SOD Activity Assay—SOD activity of whole homogenates prepared on ice following 2 freeze thaw cycles in 50 mM potassium phosphate buffer (pH 7.8, with 1.34 mM diethylenetriaminepentaacetic acid) was determined using an indirect competitive inhibition assay (17). This assay is based on the competition between SOD and an indicator molecule (nitro blue tetrazolium) for superoxide production from xanthine and xanthine oxidase, according to the method of Spitz and Oberley (17). Incubation for at least 45 min with 5 mM sodium cyanide was used to inhibit CuZn-SOD activity to measure Mn-SOD activity.

Preparation of Mitochondria—Twelve 15-cm culture dishes of PC-3 cells (transduced with AdMitCat or vector control) grown to 80% confluence were harvested and mitochondria were prepared as described previously (18).

Western Blot Analysis—To assay for catalase immunoreactive protein levels whole homogenates, intact mitochondria, and cytosolic fractions prepared as described above were sonicated at a duty cycle of 30% (50% for whole homogenates) (Sonics Vibracell, VC750) and an output control of 3 (4 for whole homogenates) for 10 s (20 s for whole homogenates), and the protein concentration was measured (Bradford method). Five to 40 μg of denatured protein was resolved on 12% SDS-PAGE and electroblotted onto nitrocellulose membranes (Bio-Rad). The membrane to measure catalase was incubated with rabbit anti-human catalase polyclonal antibody as the primary antibody (1:1,000) (Athens, Inc., Athens, GA), whereas for cytochrome *c*, the blots were incubated with rabbit anti-human cytochrome *c* polyclonal antibody as the primary antibody (1:500) (Santa Cruz), followed by incubation with horseradish peroxidase conjugated to goat anti-rabbit IgG (Sigma) as the second antibody (1:10,000) for both. Detection by the chemiluminescence reaction was carried out for 5 min using the ECL kit (Amersham Biosciences), followed by exposure to Kodak X-Omat x-ray film (Eastman Kodak).

Intracellular Prooxidant Production—Prooxidant production was determined using the oxidation-sensitive 5- (and-6)-carboxy-2′,7′-dichlorodihydrofluorescein diacetate (C-400, 10 μg/ml) and oxidation-insensitive 5- (and-6)-carboxy-2′,7′-dichlorofluorescein diacetate (C-369, 10 μg/ml) fluorescent dyes (dissolved in Me_2SO) obtained from Molecular Probes. The oxidized form of the dye acts as a control for changes in uptake, ester cleavage, and efflux, so that any changes in fluorescence seen between groups with the oxidation-sensitive dye can be directly attributed to changes in dye oxidation. Cells were treated for the indicated period and then harvested at 37 °C using trypsin, re-suspended in 37 °C glucose-free medium with or without drugs, labeled with the fluorescent dyes for 15 min at 37 °C, placed on ice, and analyzed using a FACScan flow cytometer (BD Biosciences, Mountain View, CA) (excitation 488 nm, emission 535 nm). Normal glucose levels were added to the +glucose controls (5 mM). The mean fluorescence intensity of 20,000 cells was analyzed in each sample and corrected for autofluorescence from unlabeled cells.

Hydrogen Peroxide Production—A method for estimating H_2O_2 production by monitoring the irreversible inactivation of catalase in the presence of AT was developed based on previous reports (19). PC-3 cells were infected with 50 m.o.i. AdCAT for 24 h, allowed to recover for 24 h in the absence of virus, and then placed in media in the presence and absence of glucose for 15 h. At the end of the 15-h incubation, 50 mM AT was added to the cultures and cells were harvested for catalase activity assay at 0 to 360 min of incubation. Inhibition of catalase activity was fit to a steady-state model as described previously (20). It was assumed that a transition to a new, final steady-state value of catalase activity was achieved over time according to the differential equation,

$$dA/dt = -k(A - A_f) \quad \text{(Eq. 1)}$$

where A is the catalase activity, k is a constant, and A_f is the final steady-state catalase activity detected by the assay. Solving the above differential equation, we arrive at the following expression for the catalase activity as a function of time,

$$A(t) = A_f(1 - e^{-kt}) + A_0e^{-kt} \quad \text{(Eq. 2)}$$

where A_0 is the catalase activity at time t_0. Nonlinear least-squares regression analysis of the experimental data yielded estimates for the parameters A_f, and k. Experimental data were fit to the above equation using the Levenberg-Marquardt nonlinear least-squares method (21). This method yields the estimated parameter values, along with standard errors of these estimates. One-tailed Student's t tests were used to determine statistical significance of differences in fit parameters ($p < 0.05$).

Measurement of Intracellular ATP Levels—Intracellular ATP was measured with the Bioluminescent Somatic Cell Assay Kit (Sigma) based on a described previously luciferin-luciferase assay (22, 23). Briefly, 25,000 GM00637G SV40-transformed human fibroblasts were plated per well in 24-well plates. Two days later cells were washed twice with PBS and incubated for 2 or 8 h with (+Glu) or without (−Glu) glucose in the presence of DNP (2 μM) and AntA (10 μM) in triplicate. At the time of the assay, experimental medium was aspirated off and cells received 250 μl of a 2:1:1 mixture of somatic cell releasing agent (provided in the kit), water, and culture medium (glucose and serum-free). Cells were then incubated at 37 °C for 10 min. Plates were swirled twice and 100 μl of the mixture from each well transferred into a 96-well plate, which already contained 100 μl of ATP assay mixture. Readings were obtained with a model 392 Luminoskan Ascent luminometer (ThermoLabsystems, Finland) with a 10-s delay time, a 30-s integrate time, and no pre-delay time. Results were obtained by comparison with a standard curve and normalized per mg of cellular protein as determined by the method of Bradford (24).

$NADP^+$/NADPH Measurement—Following the 24-h treatment with (+Glu) or without (−Glu) glucose, PC-3 cells were washed with PBS twice and scrape-harvested in PBS at 4 °C. After centrifugation at 320 × *g* for 5 min, cell pellets were resuspended in 150 μl of extraction buffer containing 0.1 M Tris-HCl, pH 8.0, 0.01 M EDTA, and 0.05% (v/v) Triton X-100. The cell suspension was sonicated at a duty cycle of 34% (Sonics Vibracell, VC750) for 2 min at 30-s intervals in a cup horn filled with ice water. The solution was centrifuged at 5500 × *g* for 5 min. The supernatants were collected and analyzed immediately for $NADP^+$ and NADPH using a described previously method (25). Briefly, an aliquot (50 μl) of the extract was incubated with 950 μl of extraction buffer at 37 °C for 5 min and an absorbance measurement was taken at 340 nm. This reading measures the total amount of NADPH and NADH in the sample (A_1). Another 50-μl aliquot of the extract was pre-incubated at 37 °C for 5 min in a reaction mixture containing 5.0 IU of glucose-6-phosphate dehydrogenase, 0.1 M Tris-HCl, pH 8.0, 0.01 M $MgCl_2$, and 0.05% (v/v) Triton X-100. The reaction was initiated by the addition of 5 mM glucose 6-phosphate. After incubation of the mixture at 37 °C for 5 min, absorbance measurement was taken at 340 nm. This reaction converted $NADP^+$ to NADPH (A_2). Finally, a 50-μl aliquot of the extract was preincubated at 25 °C for 5 min in a reaction mixture containing 5.0 IU of glutathione reductase, 0.1 M phosphate buffer, pH 7.6, 0.05 mM EDTA, and 0.05% (v/v) Triton X-100. The reaction was initiated by the addition of glutathione disulfide (GSSG, 5 mM) to convert NADPH to $NADP^+$. The tubes were incubated for an additional 5 min at 25 °C, and absorbance at 340 nm was determined (A_3). Subtraction of A_3 from A_1 represents the total amount of NADPH in the sample. The total amount of $NADP^+$ was calculated by subtracting the A_1 from A_2 (25). Results were obtained by comparison with a standard curve and normalized per mg of cellular protein as determined by the method of Bradford (24).

Glutathione Reductase Measurement—Following 24 h treatment with (+Glu) or without (−Glu) glucose, PC-3 cells were washed with PBS twice and scrape-harvested in PBS at 4 °C. After centrifugation at 320 × *g* for 5 min, cell pellets were resuspended in potassium phosphate (100 mM), EDTA (3.4 mM) buffer. For each sample, a mixture containing 650 μl of ddH_2O, 1500 μl of potassium/EDTA buffer, 350 μl of NADPH (0.8 mM), 100 μl of 30 mM GSSG, and 1% bovine serum albumin was incubated at 37 °C for 5 min. An aliquot (100 μl) of the cell homogenate was added to this mixture and absorbance measurement was taken at 340 nm for 5 min. Maximum linear rates for both samples and blank were used to calculate units of glutathione reductase activity as described previously based on the extinction coefficient of β-NADPH at 340 nm (26). Results were normalized per milligram of cellular protein as determined by the method of Bradford (24).

Statistical Analysis—All results are expressed as mean ± 1 S.D. For analysis limited to two groups, Student's t test was employed ($p < 0.05$). Statistical comparisons among more than 2 treatment groups were accomplished using analysis of variance and the least significant difference test ($p < 0.05$) to determine differences between individual means.

RESULTS

Mitochondrial Electron Transport Chain Blockers Enhance Glucose Deprivation-induced Cytotoxicity and Parameters Indicative of Oxidative Stress—The effect of ETCBs on glucose deprivation-induced cytotoxicity and parameters indicative of oxidative stress was determined in GM00637G SV40-transformed human fibroblasts. GM00637G cell survival decreased dramatically after 8 h of glucose deprivation in the presence of AntA, Myx, and Rot (relative to Me_2SO control), but these drugs were not toxic in the presence of glucose during this time frame (Fig. 1*A*). No cytotoxicity was seen in cells treated with DNP in the presence or absence of glucose. Glucose deprivation (8 h) in the presence of ETCBs also increased a parameter indicative of oxidative stress (GSSG) in GM00637G-transformed human fibroblasts (Fig. 1*B*). As was noted in the survival assay, the presence of DNP caused no changes in GSSG, relative to the Me_2SO control. In addition, no significant changes in ATP levels could be detected during 8 h in the presence or absence of glucose in GM00637G cells treated with AntA or DNP (Table I), supporting the hypothesis that ATP depletion was unlikely to contribute to the observed effects.

The Time Course of Increases in Cytotoxicity and GSSG during Glucose Deprivation in the Presence of AntA—Glucose deprivation of GM00637G cells in the presence of 10 μM AntA showed time-dependent (0 to 2.5 h) increases in cytotoxicity (Fig. 2). Again, 10 μM AntA was not toxic to these cells in the presence of glucose. The data in Fig. 3 show the time course of alterations in the levels of glutathione and GSSG seen during glucose deprivation of GM00637G cells in the presence of AntA. These results demonstrate a profound disruption in glutathione metabolism in the presence of AntA when glucose is omitted from the cell culture media. Fig. 3, *A* and *B*, show increases in the steady-state levels of total glutathione and GSSG induced by 0–2.5 h of glucose deprivation in the presence of AntA. These results support the hypothesis that during glucose deprivation, the metabolic demand for glutathione synthesis increased, but in the presence of AntA, cells were unable to maintain the newly synthesized glutathione in the reduced state leading to an increase in GSSG.

Fig. 3*C* shows that exposure to AntA during glucose deprivation resulted in a decrease in the ratio of GSH/GSSG during the same time as cytotoxicity was occurring (Fig. 2), indicating a metabolic shift to a more oxidizing environment that corresponded with the onset of cell death. Furthermore, in the presence of glucose the initial decrease in the GSH/GSSG ratio was followed by recovery to normal levels indicating that in the presence of glucose the cells were able to re-establish a near normal redox environment during this time frame.

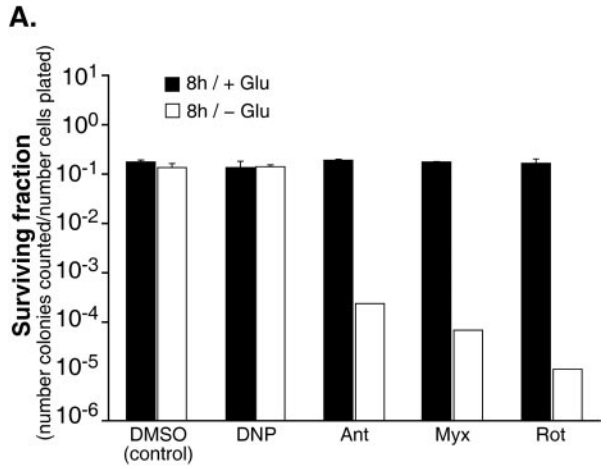

FIG. 1. **Mitochondrial electron transport chain blockers enhanced cytotoxicity and accumulation of GSSG during glucose deprivation.** GM00637G cells were incubated with (+*Glu*) or without (−*Glu*) glucose for 8 h in the presence of DNP (2 μM), Ant A (10 μM), Myx (10 μM), and Rot (50 μM). Me_2SO was included as the vehicle control. *A*, clonogenic survival, and *B*, GSSG. Errors in *panel A* represent ± 1 S.D. of at least three cloning dishes counted for each point and taken from one treatment dish. The results in *panel B* represent one measurement taken from a single culture from each group.

TABLE I
ATP levels in GM00637G cells treated with +/−Glu for 2 or 8 h (n = 3)

Group	Glucose	ATP levels	
		2 h	8 h
		nmol/mg protein	
Control	+	0.253 ± 0.015	0.249 ± 0.037
	–	0.249 ± 0.024	0.270 ± 0.001
Ant A (10 μM)	+	0.260 ± 0.026	0.306 ± 0.040
	–	0.269 ± 0.008	0.263 ± 0.023
DNP (2 μM)	+	0.273 ± 0.046	0.258 ± 0.031
	–	0.251 ± 0.025	0.231 ± 0.031

Mitochondrial Electron Transport Chain Blockers Enhance Steady-state Levels of Prooxidants during Glucose Deprivation—To test the hypothesis that ETCBs enhance steady-state levels of intracellular prooxidants (*i.e.* H_2O_2), cells were labeled with an oxidation sensitive dye during glucose deprivation. Cells deprived of glucose for 2 h in the presence of ETCBs (but not DNP) demonstrated dramatically enhanced cytotoxicity (Fig. 4*A*), as well as 3–6-fold increases in mean fluorescence intensity (MFI) when labeled with the oxidation sensitive probe

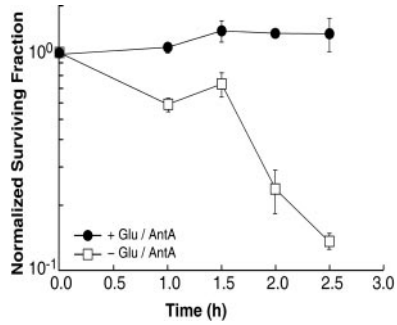

FIG. 2. **AntA induced cytotoxicity in a time dependent manner during glucose deprivation in GM00637G SV40-transformed cells.** Cells in the presence of 10 μM AntA were analyzed for clonogenic cell survival at various time intervals in the presence and absence of glucose. Errors represent ±1 S.D. of at least three cloning dishes counted for each point and taken from one treatment dish. Data were normalized to the time 0 h + glucose group.

(C-400; Fig. 4*B*). In contrast, the presence of DNP during 2 h of glucose deprivation did not affect the MFI of the cells labeled with C-400, relative to untreated or vehicle (Me_2SO)-treated cells. The MFI of cells labeled with the oxidation insensitive probe (C-369) was unchanged in the presence or absence of AntA ± glucose (Fig. 4*C*). These results clearly show that changes in MFI seen in the presence of AntA (Fig. 4*B*), when the cells were labeled with the oxidation sensitive probe were indicative of changes in quantities of the dye being oxidized, and are not changes in uptake, ester cleavage, or efflux of the probe. Therefore, increases in MFI seen in Fig. 4*B* can be interpreted as indicative of increases in steady-state levels of intracellular prooxidants during treatment with ETCBs in the absence of glucose.

Mitochondrial Electron Transport Chain Blockers Enhance Glucose Deprivation-induced Cytotoxicity and Parameters Indicative of Oxidative Stress in Several Human Cancer Cell Lines—To determine the generality of the results obtained with ETCBs in SV40-transformed human fibroblasts (Figs. 1–4), a variety of human cancer cells derived from prostate, breast, and colon were exposed to 6 h of glucose deprivation in the presence of AntA and clonogenic cell survival as well as parameters indicative of oxidative stress were assayed. PC-3, DU145, HT-29, and MDA-MB231 demonstrated significantly enhanced ($p < 0.05$) clonogenic cell killing following 6 h of glucose deprivation in the presence of AntA, relative to each respective glucose containing control (Fig. 5). Some variability in responses between the cell lines was noted with PC-3 and HT-29 showing 50% killing, MDA-MB231 showing 60% killing, and DU145 showing 90% cell killing during 6 h of glucose deprivation in the presence of AntA. These results indicate that in general, glucose deprivation-induced cytotoxicity in human cancer cells is enhanced in the presence of AntA, relative to the same cells exposed to AntA in the presence of glucose. Fig. 6 shows the results of the glutathione analysis done on co-cultures obtained from the same experiments shown in Fig. 5. Similar to what was observed with GM00637G, glucose deprivation in the presence of AntA led to significant increases in total glutathione content as well as GSSG.

Spin Trapping of Oxygen-centered Radicals during Glucose Deprivation in the Presence of AntA—To begin to identify the prooxidants formed during glucose deprivation in the presence of AntA, spin trapping of free radicals with DMPO and electron paramagnetic resonance (EPR) spectroscopy was performed. DMPO was chosen because of its low cytotoxicity, accessibility to the cell, and reaction with $^{\cdot}OH$ radicals to yield a distinctive DMPO-OH spin adduct (27–29). The reaction of DMPO with O_2^- has a lower rate constant than that with $^{\cdot}OH$ (~30 M^{-1} s^{-1}

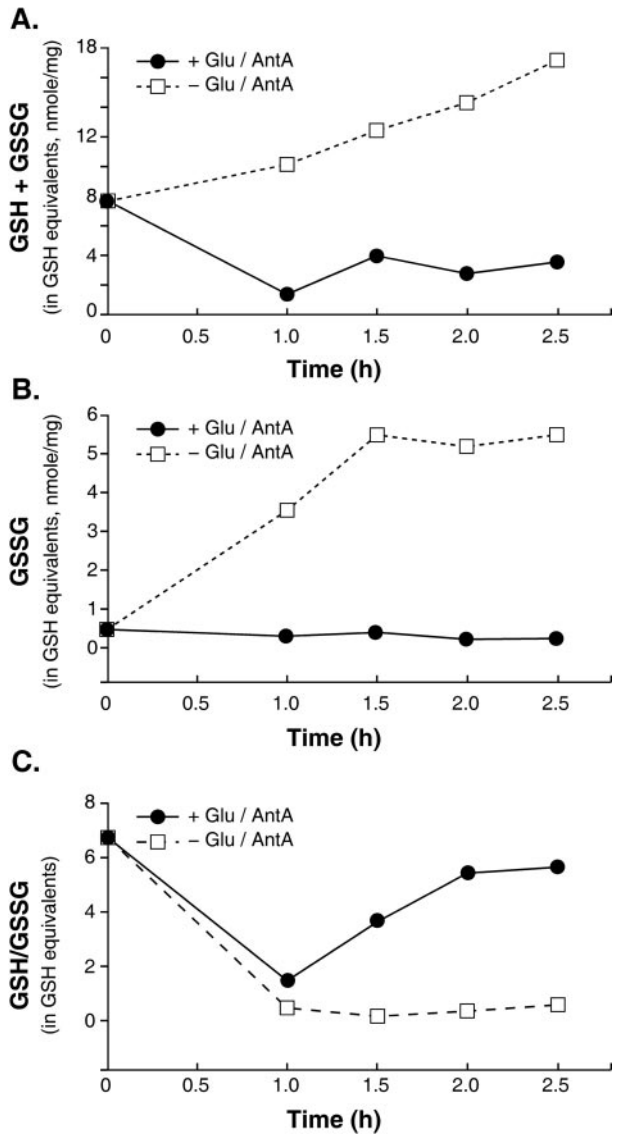

FIG. 3. **Glucose deprivation combined with AntA induced alterations in glutathione metabolism in GM00637G SV40-transformed human fibroblasts.** Cells were incubated in DMEM ± glucose and AntA (10 μM) for 0–2.5 h, and then the intracellular levels of total, oxidized, and reduced glutathione content were determined. Each data point represents a single measurement from a whole homogenate taken from a single cell culture: *A*, total glutathione content; *B*, GSSG content; and *C*, ratio of GSH/GSSG (in GSH equivalents).

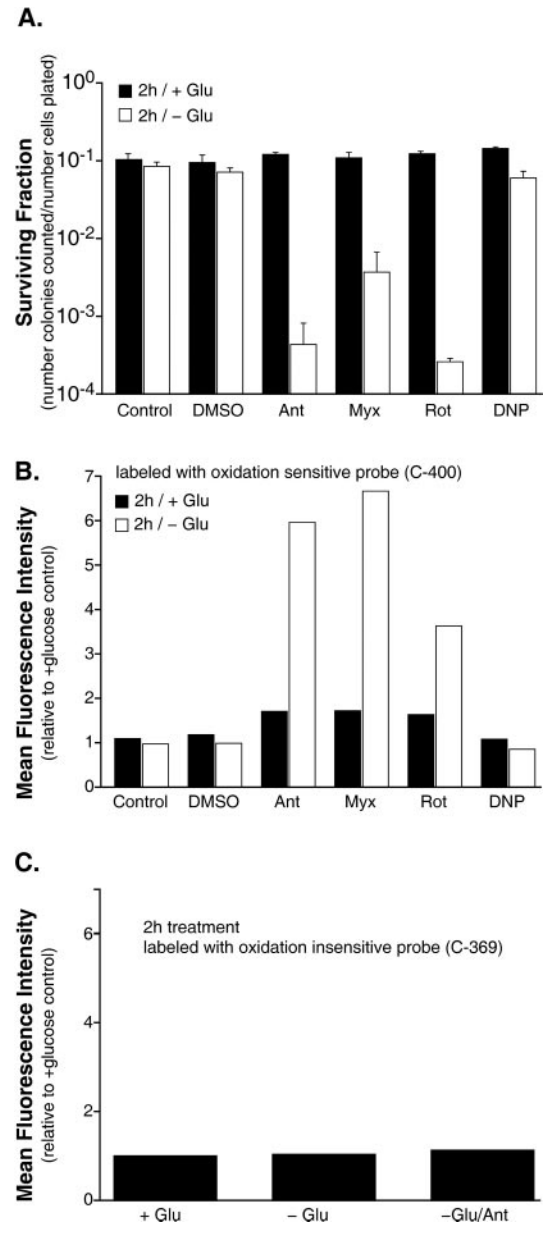

FIG. 4. **Mitochondrial electron transport chain blockers enhance steady-state levels of prooxidants during glucose deprivation.** GM00637G cells were incubated for 2 h with (+*Glu*) or without (−*Glu*) glucose in the presence of DNP (2 μM), AntA (10 μM), Myx (10 μM), and Rot (50 μM) and were examined for survival (*A*) and relative steady-state levels of prooxidants using the C-400 oxidation sensitive fluorescent dye (*B*). MFI of 20,000 cells analyzed by flow cytometry is shown. MFI was not different in glucose-deprived and glucose replete cells when labeled with the non-oxidation sensitive dye C-369 in the presence and absence of AntA (*C*) showing that changes in MFI in *panel B* are indicative of changes in steady-state levels of dye oxidation. Errors represent ±1 S.D. of at least three cloning dishes taken from a single cell culture.

at pH 7 (30)) and yields a product (DMPO-OOH) that is converted to DMPO-OH by GPx (31). This makes DMPO a useful probe for detecting oxygen-centered radicals arising from O_2^- and H_2O_2. GM00637G cells (7×10^6) were used to evaluate steady-state levels of oxygen-centered radicals during glucose deprivation in the presence of AntA using DMPO (Fig. 7). In the absence of glucose a clearly evident EPR signal consisting of the 1:2:2:1 quartet typical of the DMPO-OH spin adduct with a hyperfine splitting equal to $a^N = a^H = 14.36$ Gauss was observed (30). This experiment was repeated three times and similar results were obtained. The results in Fig. 7 clearly show increased steady-state levels of oxygen-centered radicals during glucose deprivation in the presence of AntA, but the precise identity of the radical could be either O_2^- and/or $^{\cdot}OH$.

Glucose Deprivation-induced Cytotoxicity and Oxidative Stress in Cells Lacking Functional Mitochondrial Electron Transport Chains—To provide further support for the involvement of mitochondrial electron transport chain activity in glucose deprivation-induced cytotoxicity and oxidative stress, human osteosarcoma cells deficient in fully functional mitochondrial electron transport chains by virtue of completely lacking mitochondrial DNA were utilized (10, 32). Fig. 8 shows clonogenic cell survival data from mitochondrial deficient rho(0) and the parental rho(+) cells during 6 and 8 h of glucose deprivation (using DMEM) in the presence of AntA. Rho(+) cells demonstrated 40 and 70% cell killing during 6 and 8 h of glucose deprivation, respectively, in the presence of AntA (Fig. 8*A*). In contrast, rho(0) cells exhibited 20 and 30% cell killing during the same time frame in the presence of AntA (Fig. 8*B*).

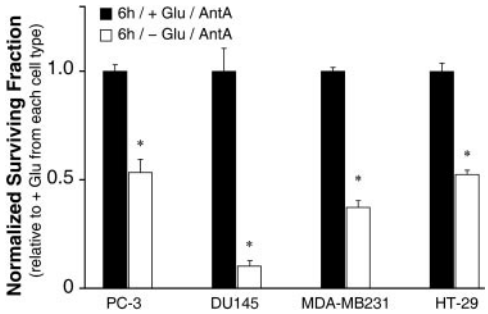

FIG. 5. **Clonogenic cell survival showed increased susceptibility of human cancer cells (PC-3, DU145, MDA-MB231, and HT29) to glucose deprivation-induced cytotoxicity in the presence of AntA.** Cells were exposed for 6 h in DMEM ± glucose in the presence of 10 μM AntA. Errors represent ±1 S.D. *Asterisks* indicate significant differences between +Glu and −Glu from each cell line ($p < 0.05$, t test, $n = 3$). Data were normalized to sham treated cultures from each cell line.

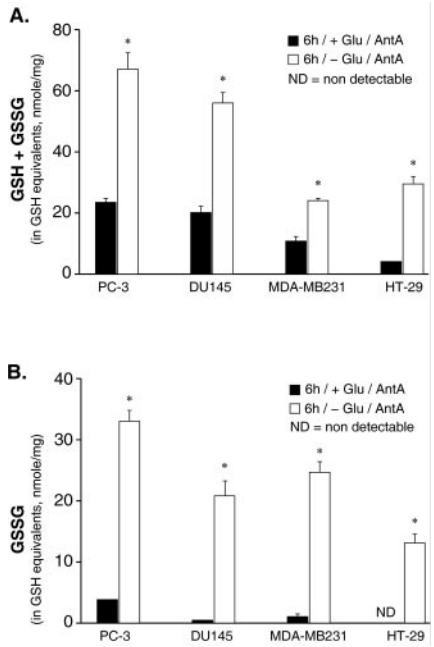

FIG. 6. **Total glutathione and GSSG were increased in human cancer cells (PC-3, DU145, MDA-MB231, and HT29) exposed to glucose deprivation combined with AntA for 6 h.** Cells were incubated +*Glu* or −*Glu* in the presence of 10 μM AntA for 6 h and then the intracellular levels of total and oxidized glutathione were determined. *A*, total glutathione content; and *B*, GSSG content. Errors represent ±1 S.D. *Asterisks* indicate significant differences between +Glu and −Glu from each cell line ($p < 0.05$, t test, $n = 3$).

Furthermore, following 6 or 8 h of glucose deprivation in the presence of AntA, GSSG and % GSSG (moles of GSH in the form of GSSG/mol of total GSH + GSSG) was greater in rho(+) cells, relative to rho(0) cells (Tables II and III). These results support the hypothesis that fully functional mitochondrial electron transport chains significantly contribute to glucose deprivation-induced cytotoxicity and oxidative stress in human cancer cells.

Estimation of Steady-state Levels of H_2O_2 during Glucose Deprivation in the Absence of ETCBs—To specifically estimate differences in steady-state levels of intracellular H_2O_2 fluxes during glucose deprivation, a method based on the stoichiometric interaction of H_2O_2 with catalase in the presence of AT leading to the irreversible inhibition of catalase enzymatic activity was developed from literature reports (19). Catalase specifically binds one molecule of H_2O_2 leading to the formation of one molecule of the Compound I form of catalase as an intermediate (19). Compound I can then covalently interact with one molecule of AT leading to the irreversible inhibition of catalase activity as demonstrated in Scheme 1 (19). By moni-

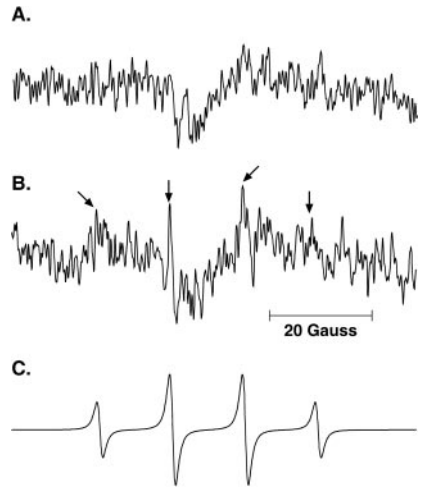

FIG. 7. Increased oxygen-centered radical formation as detected using EPR spectra of the DMPO-OH spin adduct obtained from SV40 GM00637G-transformed cells treated in the presence (*A*) and absence (*B*) of glucose with 10 μM AntA. Freshly trypsinized cells (7×10^6), washed twice and re-suspended in PBS, were treated 10 min ±glucose with 10 μM AntA at 37 °C. Cells were then incubated at 37 °C with 100 mM DMPO for another 15 min and EPR measurements were performed at room temperature. The spectra collected represent the signal average of 15 scans. The hyperfine splitting of the DMPO-OH adduct has value of $a^N = a^H = 14.36$ G consistent with the formation of DMPO/˙OH. *C* is a simulation of a DMPO-OH EPR spectrum obtained when DMPO traps ˙OH radicals.

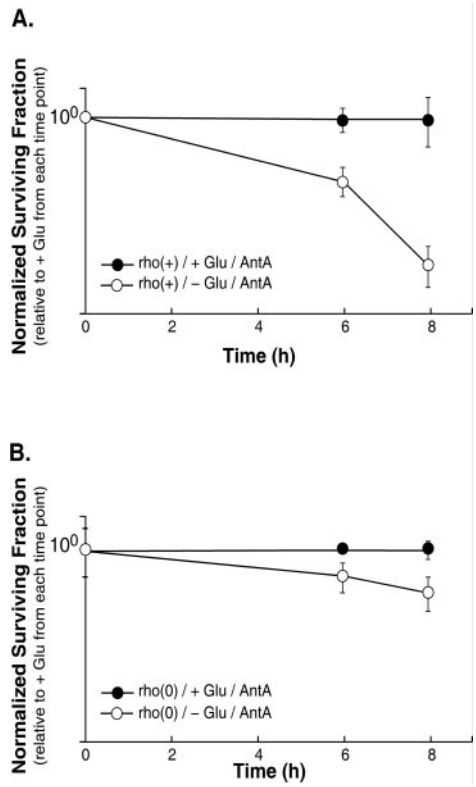

FIG. 8. **Rho(+) cells (*A*) were more susceptible to glucose deprivation-induced cytotoxicity in the presence of AntA as compared with rho(0) cells (*B*).** Control (+*Glu*) or glucose-deprived (−*Glu*) cells in the presence of 10 μM AntA were analyzed for clonogenic cell survival (y axis range, 1.0−0.2; $\log_{10}$). Errors represent ±1 S.D. of at least three cloning dishes counted for each point and taken from one treatment dish.

TABLE II
Glutathione analysis of rho(0) versus rho(+) osteosarcoma cells treated with +/−Glu and 10 μM Ant A for 6 h

Osteosarcoma cells	Glucose	Total GSH	GSSG[a]	% GSSG[b]
		nmol/mg		
Rho(+)	+	7.5	0.3	3.9
	−	5.6	1.1	20.0
Rho(0)	+	15.6	0.9	6.0
	−	6.4	0.0	0.0

[a] GSSG is expressed in GSH equivalents.
[b] % GSSG = (GSSG/Total GSH × 100).

TABLE III
Glutathione analysis of rho(0) versus rho(+) osteosarcoma cells treated with +/−Glu and 10 μM AntA for 8 h

Osteosarcoma cells	Glucose	Total GSH	GSSG[a]	% GSSG[b]
		nmol/mg		
Rho(+)	+	7.2	0.6	8.3
	−	7.3	1.7	23.7
Rho(0)	+	11.4	0.4	3.2
	−	6.6	0.5	8.0

[a] GSSG is expressed in GSH equivalents.
[b] % GSSG = (GSSG/total GSH × 100).

$$H_2O_2 + \text{catalase} \rightarrow \text{compound I}$$

$$\text{Compound I} + \text{AT} \rightarrow \text{inactive catalase}$$

SCHEME 1. AT-mediated inactivation of catalase.

toring the rate of disappearance of catalase activity in the presence of AT during different experimental conditions, changes in steady-state levels of intracellular H_2O_2 can be readily detected (19). Because endogenous catalase activity in the PC-3 cells is fairly low, initially the cells were transduced with AdCAT to increase catalase activity 20–40-fold. Then cells were glucose deprived for 15 h, after which AT was added to the cultures and the inhibition of catalase activity monitored as a function of time for 6 h in the absence of ETCBs (Fig. 9). The rate constant for catalase inhibition by AT was significantly greater ($p < 0.01$) in the absence of glucose ($k = 9.03 \times 10^{-3} \pm 7.84 \times 10^{-5}$ s^{-1}), relative to cells in the presence of glucose ($k = 7.69 \times 10^{-3} \pm 8.37 \times 10^{-5}$ s^{-1}) supporting the hypothesis that steady-state concentrations of H_2O_2 were greater during glucose deprivation in these human cancer cells. In an attempt to provide an estimate of steady-state H_2O_2 concentrations using the data in Fig. 9, a system of differential equations was constructed using the reactions shown in Scheme 1. In construction of this model, it was assumed that the first step, formation of Compound I, and the last step, production of inactive catalase, were essentially irreversible. These assumptions have been used in the past (19). We also assumed that the production of Compound I achieved a steady-state very rapidly, implying that the Compound I produced by the first step in Scheme 1 combined with AT as fast as it was formed, as AT was assumed to be in excess in this reaction. Using the steady-state model for catalase inactivation described above, an estimate of the intracellular H_2O_2 concentration at the start of the experiment was obtained through solution of the set of differential equations. From this analysis for the experiment that is shown in Fig. 9 estimates of intracellular steady-state H_2O_2 concentrations of 4.4 pM in the presence of glucose and 5.8 pM in the absence of glucose were obtained. We conclude based on this analysis and the rate constants for catalase inhibition by AT presented above, that glucose deprivation increased steady-state concentrations of H_2O_2 in these human cancer cells.

$NADP^+$/NADPH Levels and Glutathione Reductatse Activity in PC-3 Cells during Glucose Deprivation—Our hypothesis

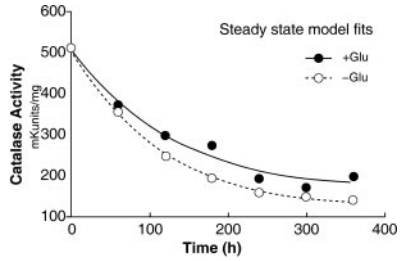

FIG. 9. **Increased steady-state levels of intracellular H_2O_2 in glucose-deprived PC-3 cells**. Intracellular H_2O_2 levels were estimated in PC-3 cells using AT-mediated inactivation of catalase. PC-3 cells overexpressing catalase activity following transduction with Ad-CAT were deprived of glucose for 15 h prior to the addition of 50 mM aminotriazole for 0–360 min. At each time point the cells were scrape-harvested and catalase activity (milli-*k* units/mg) was determined in the cell homogenates obtained from each sample. The equation used to fit the data points is: $A(t) = A_f(1 - e^{-kt}) + A_0e^{-kt}$, where A is the catalase activity at time t, k is a rate constant, A_f is the final steady-state catalase activity, and A_0 is the initial catalase activity. The rate constant (k) for catalase inhibition in −Glu was significantly greater than in +Glu ($p < 0.01$).

would predict that during glucose deprivation, the cells' ability to metabolize hydroperoxides via glutathione peroxidase and peroxiredoxin enzymes would be compromised based on the fact that glucose would be unavailable for metabolism in the pentose cycle to allow for the regeneration of NADPH from $NADP^+$. If glutathione peroxidase and peroxiredoxin enzymes were significantly contributing to hydroperoxide removal, the loss in ability to regenerate NADPH during glucose deprivation could account for the increase in steady-state levels of H_2O_2 noted in Fig. 9. To determine whether regeneration of NADPH was compromised during glucose deprivation, NADPH/$NADP^+$ analysis was accomplished on PC-3 cells exposed to 24 h of glucose deprivation in the absence of ETCBs (Table IV). The results in Table IV show that NADPH levels were significantly reduced and the ratio of $NADP^+$/NADPH was significantly increased during glucose deprivation. The results in Table V show that this effect on NADPH levels was not related to decreased glutathione reductase activity during glucose deprivation. Overall the results in Tables IV and V are consistent with the hypothesis that glucose deprivation induces a significant decline in the availability of NADPH to recycle glutathione disulfide (and also oxidized thioredoxin) to the reduced state. Therefore the ability of the glutathione peroxidase (and also peroxiredoxins) to decompose H_2O_2 is most likely compromised during glucose deprivation and this could contribute to the apparent increases in steady-state levels of H_2O_2 noted in Fig. 9.

Overexpression of Catalase Containing a Mitochondrial Leader Sequence—To verify our ability to use adenoviral vectors to increase the capacity of mitochondria to metabolize H_2O_2, PC-3 human prostate carcinoma cells were transduced with 50 m.o.i. of AdBglII (empty vector), or an adenovirus containing human catalase cDNA with a 80-bp Mn-SOD mitochondrial leader sequence (AdMitCat) and assayed for immunoreactive catalase protein. Fig. 10 shows the expression of catalase (as determined by immunoblotting) in the cytosolic extract (*lanes 1* and *2*), and in the mitochondrial extract (*lanes 3* and *4*). Results from densitometric analysis of the intensity of the various bands indicated that the expression of immunoreactive catalase in cytosolic extracts of cells transduced with AdMitCat (*lane 2*) was greater than 2-fold increased, relative to cells transduced with empty vector (*lane 1*). A greater than 2-fold increase in the amount of immunoreactive catalase was also found in the mitochondrial extracts of the AdMitCat-transduced PC-3 cells (*lane 4*), relative to the control (*lane 3*). The same extracts were analyzed for immunoreactive cytochrome *c*

TABLE IV
NADP+/NADPH levels in PC-3 cells treated with +/−Glu for 24 h (n = 3)

Group	NADP+	NADPH	$NADP^+$/NADPH
	nmol/mg protein		*ratio*
Glucose +	70.5 ± 1.8	32.1 ± 2.3	2.2 ± 0.1
Glucose −	27.4 ± 0.4[a]	4.5 ± 1.4[a]	6.4 ± 1.6[a]

[a] $p < 0.05$ compared with corresponding glucose + group.

TABLE V
Glutathione reductase activity in PC-3 cells ± Glu for 24 h (n = 3)

Group	GR
	milliunits/mg protein
Glucose +	6.04 ± 0.29
Glucose −	9.97 ± 0.60[a]

[a] $p < 0.05$ compared with corresponding glucose + group.

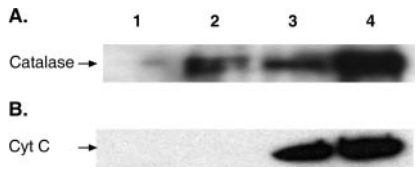

FIG. 10. **Expression of immunoreactive catalase in AdMitCat-transduced PC-3 human prostate carcinoma cells.** Five micrograms of protein from cellular extracts (*lanes 1* and *2*), or from mitochondrial extracts (*lanes 3* and *4*) were loaded into each lane for 12% SDS-PAGE, followed by immunoblot analysis with polyclonal rabbit anti-human catalase antibody as described under "Experimental Procedures" (*A*). Forty μg of protein from both extracts were loaded for immunoblotting using antibody to cytochrome *c* (*B*). *Lane 1*, cytosolic extract from cells transduced with empty vector. *Lane 2*, cytosolic extract from cells transduced with 50 m.o.i. AdMitCat. *Lane 3*, mitochondrial extract from cells transduced with empty vector. *Lane 4*, mitochondrial extract from cells transduced with AdMitCat.

as a molecular marker specific for mitochondria. As shown in Fig. 10, cytochrome *c* was detected only in the mitochondrial extracts. These results indicate that AdMitCat transduction was effective at increasing expression of immunoreactive catalase protein in both the mitochondrial and cytosolic fractions of PC-3 cells. This was the expected result, because the construct contained both the peroxisomal as well as the mitochondrial targeting sequences (15).

The Effect of Mn-SOD and/or MitCat Overexpression on Glucose Deprivation-induced Cytotoxicity and Parameters Indicative of Oxidative Stress in the Absence of ETCBs—To determine whether increased steady-state levels of O_2^- and H_2O_2 were causally involved with glucose deprivation-induced cytotoxicity and oxidative stress, human prostate cancer cells (PC-3) were transduced with 10 and 50 m.o.i. of AdMn-SOD and/or AdMitCat, respectively, and then treated in the presence and absence of glucose. The results in Table VI demonstrate in this experiment a ~10-fold change in either or both enzymatic activities induced by this treatment with the adenoviral vectors. The results in Fig. 11*A* demonstrate that overexpression of Mn-SOD and/or MitCat activity partially protected PC-3 cells from clonogenic inactivation induced by 48 h of glucose deprivation, but when both enzymes were overexpressed, significantly more protection was seen than with either enzyme alone (*, $p < 0.001$). The results in Fig. 11*B* show that overexpression of either antioxidant enzyme alone slightly suppressed GSSG accumulation by ~20% during glucose deprivation, relative to the appropriate vector control. In contrast, those cultures overexpressing both Mn-SOD and MitCat demonstrated significantly greater (~50%) suppression in the accumulation of GSSG during glucose deprivation than cells overexpressing either enzyme alone, relative to the appropriate vector control (**, $p < 0.01$). These results provide strong evidence that both mitochondrial

TABLE VI
Catalase and Mn-SOD activity in PC-3 cells transduced with 50 m.o.i. AdMitCat or 10 m.o.i. AdMn-SOD or both and treated ± Glu for 48 h

Group	Glucose	Catalase activity	Mn-SOD activity
		milli-k unit/mg	*units/mg*
AdBgl II (60 m.o.i.)	+	16	5
	−	10	5
AdMitCat (50 m.o.i.)	+	101	12
	−	122	16
AdMn-SOD (10 m.o.i.)	+	12	71
	−	14	83
AdMitCat/Mn-SOD (50/10 m.o.i.)	+	106	111
	−	143	125

O_2^- and H_2O_2 contribute to the cytotoxicity and oxidative stress associated with glucose deprivation in this model system.

DISCUSSION

Pathways associated with cancer cell energy metabolism deviate significantly from those of normal tissues. Cancer cells maintain high aerobic glycolytic rates and produce high levels of lactate and pyruvate (4, 33). This phenomenon first described over 70 years ago is known as the Warburg effect (4, 33). Tumor cells have been suggested to have an aberrant respiratory mechanism, which could possibly lead to the generation of excess O_2^- and H_2O_2 by mitochondria (1–3). An increase in glucose metabolism has been hypothesized to be necessary for cancer cells to survive the potentially lethal effects of prooxidant production during respiration (3), because glucose metabolism gives rise to pyruvate and NADPH both of which are believed to function in hydroperoxide detoxification. Recently it was discovered that simply removing glucose from cell culture medium induces cytotoxicity and increases in parameters indicative of oxidative stress in human tumor cells (reviewed in Ref. 3). Because mitochondrial metabolism would be the preferred route of energy production during glucose deprivation, we hypothesized that mitochondrial production of reactive oxygen species (O_2^- and H_2O_2) mediates the susceptibility of human cancer cells to glucose deprivation-induced metabolic oxidative stress and cytotoxicity.

Historically, ETCBs have been utilized to determine the various complexes in isolated mitochondria that produce O_2^- and H_2O_2 (34–37). In general, isolated mitochondria have been shown to increase their production of O_2^- when exposed to different ETCBs such as AntA, Myx, and Rot (34–37), but very little of this work has been done in intact cells or human cancer cells. AntA is thought to inhibit the transfer of electrons from cytochrome *b* to coenzyme Q on the matrix side of the inner mitochondrial membrane and therefore could lead to increased O_2^- production from ubisemiquinone ($Q^{\cdot}$) in complex III, the FMN in complex I, as well as the FAD site in complex II (Fig. 12). Myx prevents the transfer of electrons from the hydroquinone (QH_2) to FeS(III) protein and then to cytochrome *c* (36) (Fig. 12). This is believed to effectively eliminate O_2^- production from ubisemiquinone while allowing for O_2^- production at complexes I and II (Fig. 12). Rotenone is a specific blocker of NADH dehydrogenase activity in the mitochondrial electron transport chain at site I, but does not block the flow of electrons from complex II to complex III (Fig. 12) (38). The proton ionophore DNP has been found to uncouple electron transport and ATP synthesis without blocking electron flow and was included as a control (38).

The current study shows glucose deprivation-induced cytotoxicity and oxidative stress in human tumor cells is clearly enhanced in the presence of ETCBs as evidenced by profound disruptions in the steady-state levels of total glutathione (GSH + GSSG) and GSSG accumulation followed by clonogenic

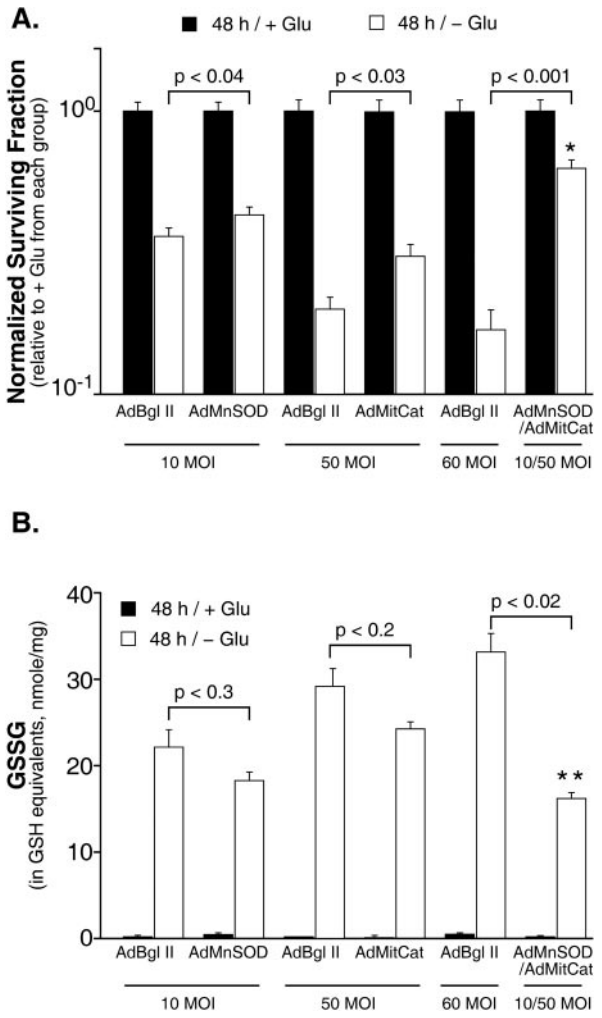

FIG. 11. **Transduction of PC-3 cells with AdMn-SOD and/or AdMitCat suppressed the cytotoxicity and GSSG accumulation induced by 48 h of glucose deprivation.** PC-3 cells were exposed to 10 m.o.i. AdMn-SOD and/or 50 m.o.i. AdMitCat 24 h after plating. The media was changed 24 h after the virus addition and replaced with fresh media. Cells were then treated with ±Glu for 48 h. Errors represent ±1 S.D. of three experiments. Survival data were normalized to sham treated cultures from each time point. *A*, clonogenic cell survival, and *B*, GSSG. The differences between glucose-deprived vector control groups *versus* glucose-deprived vector containing antioxidant groups were determined using Student's *t* test and the *p* values for each comparison are specified *above* the lines pointing to the groups being compared ($n = 3$). Comparisons of protective effects when both vectors were used together *versus* results obtained when each vector was used alone were made using analysis of variance and the least significant difference test (*, $p < 0.001$; **, $p < 0.01$, $n = 3$).

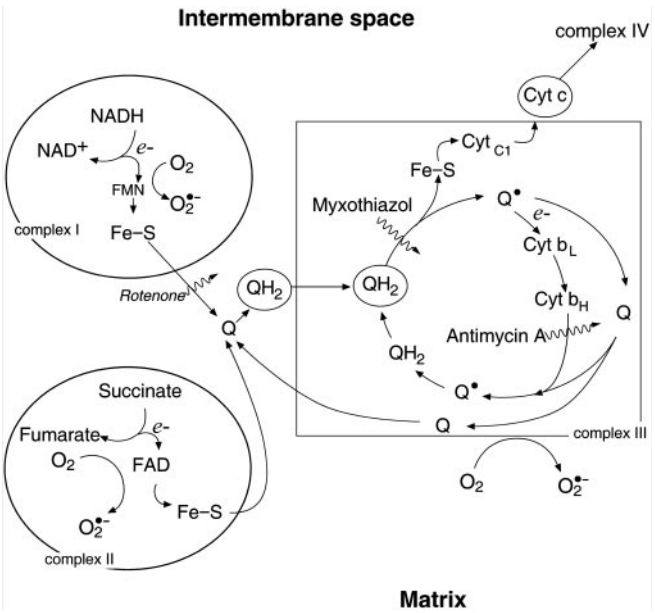

FIG. 12. **Scheme showing the possible sites of O_2^- production in the mitochondrial respiratory chain (modified from Ref. 38).** The *curved arrows* show the proposed sites of one-electron reductions of O_2 in the presence of the various blockers. For every $2QH_2$ that enters the Q cycle, $1QH_2$ is regenerated.

cell killing (Figs. 1–6). This suggests that cancer cells exposed to glucose deprivation in the presence of ETCBs are increasing glutathione synthesis in an attempt to counteract increases in steady-state levels of intracellular prooxidants, presumably hydroperoxides. In addition, it is clear that during glucose deprivation the increase in glutathione content is not sufficient to counteract the prooxidant production as evidenced by the significant increases in GSSG (Fig. 1*B*) and significantly enhanced cytotoxicity (Fig. 1*A*). It is reasonable to assume that increases in GSSG content seen in glucose-deprived human cancer cells in the presence of ETCBs derives from mitochondrial production of hydroperoxides that exceeds the metabolic capability of the glutathione peroxidase/glutathione reductase system to maintain glutathione in the reduced form. This hypothesis was further tested by measuring prooxidant production with an oxidation sensitive dye after glucose deprivation for 2 h in the presence of ETCBs (Fig. 4). An increase in steady-state levels of prooxidants and cytotoxicity was again confirmed using this methodology.

Because AntA is well known to increase O_2^- as well as H_2O_2 production in studies using isolated mitochondria from normal tissues (34), it was chosen for further studies to determine the possible role of mitochondrial O_2^- and H_2O_2 in glucose deprivation-induced cytotoxicity and oxidative stress. In the presence of AntA, EPR spin trapping using DMPO showed increased steady-state levels of oxygen-centered radicals when SV40-transformed human cells were glucose deprived (Fig. 7). This EPR signal could arise from either O_2^- or $^{\bullet}OH$. The results of survival analysis (Figs. 1–5) as well as the prooxidant measurements and EPR results (Fig. 7) support the hypothesis that mitochondrial electron transport chains are sites of prooxidant production during glucose deprivation, and that O_2^- and/or H_2O_2 are involved.

To further investigate the involvement of mitochondria in glucose deprivation-induced cytotoxicity and oxidative stress in human cancer cells, human osteosarcoma cells containing fully functional mitochondria (rho(+)) were compared with the same cells lacking functional mitochondria (rho(0)). Rho(+) cells were found to be more sensitive to glucose deprivation-induced cytotoxicity and increases in parameters indicative of oxidative stress in the presence of AntA as compared with rho(0) (Fig. 8, Tables II and III). These results support the notion that fully functional mitochondrial electron transport chains significantly contribute to glucose deprivation-induced cytotoxicity and oxidative stress in human cancer cells.

To determine whether increases in steady-state levels of H_2O_2 occurred during glucose deprivation in the absence of ETCBs, intracellular H_2O_2 fluxes were estimated in glucose-deprived human prostate cancer cells (PC-3) using AT-mediated inactivation of catalase. AT leads to irreversible inhibition of catalase activity by covalently interacting with Compound I (19). Because the only known molecule capable of converting catalase to Compound I is H_2O_2, this method provides a very specific estimate of steady-state H_2O_2 fluxes inside cells. Experiments using AT-mediated inactivation of catalase indi-

cated a significant increase in steady-state levels of intracellular H_2O_2 in PC-3 cells during glucose deprivation (Fig. 9). Surprisingly, when steady-state concentrations of intracellular H_2O_2 based on this method were calculated, they were found to be in the picomolar rather than in the nanomolar range. This was unexpected based on previous estimates done in samples of liver tissue (19). There are several possible reasons for this apparent discrepancy. First, the cells used in the current study are prostate cancer cells, which have not been studied extensively, and it is possible that they have substantially lower steady-state levels of H_2O_2 than liver cells. Second, it is possible that the detectable levels of intracellular H_2O_2 were low because the method utilized involved the dramatic overexpression of catalase following infection with the AdCAT vector. Finally, it is possible that the intracellular compartmentalization of catalase relative to the aminotriazole may have resulted in limited accessibility of catalase to aminotriazole that could have resulted in lower estimates of H_2O_2 concentration. Efforts are underway to confirm the validity of these numerical estimates of absolute H_2O_2 concentration using independent verification with other methods. However, we feel this methodology is sufficiently rigorous to support the conclusion that steady-state levels of H_2O_2 are elevated during glucose deprivation in PC-3 cells.

To determine whether glucose deprivation in the absence of ETCBs compromised the cells ability to regenerate NADPH from $NADP^+$ (as predicted by our hypothesis), analysis of NADPH/$NADP^+$ was accomplished in glucose-deprived PC-3 cells (Table IV). Consistent with our hypothesis, NAPDH levels were significantly reduced during glucose deprivation (Table IV) confirming the notion that H_2O_2 metabolism via NADPH-dependent peroxidase pathways was compromised during glucose deprivation in the same time frame that steady-state levels of H_2O_2 were shown increase (Fig. 9).

Finally, superoxide (Mn-SOD) and hydrogen peroxide (catalase) metabolizing enzymes were overexpressed in the mitochondria of PC-3 cells to determine the causal involvement of these species in glucose deprivation-induced cytotoxicity and oxidative stress in the absence of ETCBs. The results of this work show that MitCat and Mn-SOD were capable of partially inhibiting the glucose deprivation-induced cytotoxicity and oxidative stress in PC-3 cells (Fig. 11). Furthermore, when both enzymes were overexpressed, more inhibition of glucose deprivation-induced cytotoxicity and GSSG accumulation was noted than with either enzyme alone. These results suggest that both O_2^- and H_2O_2 were participating in the reactions leading to cytotoxicity and increases in steady-state levels of GSSG during glucose deprivation. Furthermore, because O_2^- is an excellent reductant for redox active metal ions such as Fe^{3+} that catalyze the formation of $^{\cdot}OH$ from H_2O_2 (39), these results also suggest that the iron-catalyzed Haber-Weiss reaction may significantly contribute to glucose deprivation-induced cytotoxicity and oxidative stress. Interestingly, overexpression of the cytosolic form of the superoxide dismutase enzyme (CuZn-SOD) using a similar adenovirus vector showed no inhibition of clonogenic inactivation or oxidative stress induced by glucose deprivation in PC-3 cells (data not shown). This result is also consistent with the mitochondrial production of superoxide being most important for the cytotoxic effects of glucose deprivation.

Overall, the results of this study strongly support the hypothesis that during glucose deprivation mitochondrial O_2^- and H_2O_2 significantly contribute to cytotoxicity and increases in parameters indicative of oxidative stress in human cancer cells. These results also support the hypothesis that O_2^--mediated reduction of redox active metal ions (such as Cu^{2+} and Fe^{3+}), combined with increased metabolic fluxes of H_2O_2 undergoing Fenton chemistry to generate $^{\cdot}OH$, significantly contributes to glucose deprivation-induced cytotoxicity and oxidative stress. Because alterations in glucose metabolism are widely observed in human cancers, a detailed understanding of the mechanisms by which glucose deprivation induces cytotoxicity and oxidative stress in cancer cells may prove useful in the development of biochemical rationales for novel therapeutic interventions for the treatment of cancer.

Acknowledgments—We thank Dr. Michael King (Thomas Jefferson University, Philadelphia, PA) for kindly providing the human osteosarcoma 143BTK− rho(+) and rho(0) cells, Dr. Mary Hendrix (University of Iowa, Iowa City, IA) for providing human breast carcinoma cells, and Dr. Andre Melendez (Albany Medical College, Albany, NY) for providing the cDNA construct with catalase fused to the mitochondrial leader sequence of Mn-SOD.

REFERENCES

1. Oberley, L. W., and Buettner, G. R. (1979) *Cancer Res.* **39,** 1141–1149
2. Oberley, T. D., and Oberley, L. W. (1993) in *Free Radicals in Aging* (Yu, B. P., ed) CRC Press, Boca Raton, FL
3. Spitz, D. R., Sim, J. E., Ridnour, L. A., Galoforo, S. S., and Lee, Y. J. (2000) *Ann. N. Y. Acad. Sci.* **899,** 349–362
4. Warburg, O. (1956) *Science* **132,** 309–314
5. Nath, K. A., Ngo, E. O., Hebbel, R. P., Croatt, A. J., Zhau, B., and Nutter, L. M. (1995) *Am. J. Physiol.* **268,** C227–C236
6. Averrill-Bates, D. A., and Przybytkowski, E. (1994) *Arch. Biochem. Biophys.* **312,** 52–58
7. Lee, Y. J., Galoforo, S. S., Berns, C. M., Chen, J. C., Davis, B. H., Sim, J. E., Corry, P. M., and Spitz, D. R. (1998) *J. Biol. Chem.* **273,** 5294–5299
8. Blackburn, R. V., Spitz, D. R., Liu, X., Galoforo, S. S., Sim, J. E., Ridnour, L. A., Chen, J. C., Daris, B. H., Corry, P. M., and Lee, Y. J. (1999) *Free Radic. Biol. Med.* **26,** 419–430
9. Hendrix, M. J., Seftor, E. A., Seftor, R. E., and Trevor, K. T. (1997) *Am. J. Pathol.* **150,** 483–495
10. King, M. P., and Attardi, G. (1996) *Methods Enzymol.* **264,** 304–313
11. Spitz, D. R., Malcolm, R. R., and Roberts, R. J. (1990) *Biochem. J.* **267,** 453–459
12. Lowry, O. H., Rosebrough, N. J., Farr, A. L., and Randall, R. J. (1951) *J. Biol. Chem.* **193,** 265–275
13. Buettner, G. R., and Kiminyo, K. P. (1992) *J. Biochem. Biophys. Meth.* **24,** 147–151
14. Zwacka, R. M., Dudus, L., Epperly, M. W., Greenburger, J. S., and Engelhardt, J. F. (1998) *Hum. Gene Ther.* **9,** 1381–1386
15. Bai, J., Rodriquez, A. M., Melendez, J. A., and Cederbaum, A. I. (1999) *J. Biol. Chem.* **274,** 26217–26224
16. Spitz, D. R., Elwell, J. H., Sun, Y., Oberley, L. W., Oberley, T. D., Sullivan, S. J., and Roberts, R. J. (1990) *Arch. Biochem. Biophys.* **279,** 249–260
17. Spitz, D. R., and Oberley, L. W. (1989) *Anal. Biochem.* **179,** 8–18
18. Dobson, A. W., Xu, Y., Kelley, M. R., LeDoux, S. P., and Wilson, G. L. (2000) *J. Biol. Chem.* **278,** 37518–37523
19. Chance, B., Sies, H., and Boveris, A. (1979) *Physiol. Rev.* **59,** 527–605
20. Mackey, M. A., and Roti Roti, J. L. (1992) *J. Theor. Biol.* **156,** 133–146
21. Press, W. H., Flannery, B. P., Teukolsky, S. A., and Vetterling, W. T. (1988) *Numerical Recipes in C*, Cambridge University Press, New York
22. Stanley, P. E. (1986) *Methods Enzymol.* **133,** 14–22
23. Singh, G., Lakkis, C. L., Laucirica, R., and Epner, D. E. (1999) *J. Cell. Physiol.* **180,** 431–438
24. Bradford, M. A. (1976) *Anal. Biochem.* **72,** 248–256
25. Zhang, Z., Yu, J., and Stanton, R. C. (2000) *Anal. Biochem.* **285,** 163–167
26. Mavis, R. D., and Stellwagen, E. (1968) *J. Biol. Chem.* **243,** 809–814
27. Green, M. R., Hill, H. A., Okolow-Zubkowska, M. J., and Segal, A. W. (1979) *FEBS Lett.* **100,** 23–26
28. Rosen, G. M., and Freeman, B. A. (1984) *Proc. Natl. Acad. Sci. U. S. A.* **81,** 7269–7273
29. Finkelstein, E., Rosen, G. M., and Rauckman, E. J. (1980) *Arch. Biochem. Biophys.* **200,** 1–16
30. Finkelstein, E., Rosen, G. M., Rauckman, E. J., and Paxton, J. (1979) *Mol. Pharmacol.* **16,** 676–685
31. Finkelstein, E., Rosen, G. M., and Rauckman, E. J. (1982) *Mol. Pharmacol.* **21,** 262–265
32. Gray, M. W. (1989) *Annu. Rev. Biochem.* **5,** 25–50
33. Galarraga, J., Loreck, D. J., Graham, J. F., DeLaPaz, R. L., Smith, B. H., Hallgren, D., and Cumins, C. J. (1986) *Metab. Brain Dis.* **1,** 279–291
34. Boveris, A. (1977) *Adv. Exp. Med. Biol.* **78,** 67–82
35. Boveris, A., and Cadenas, E. (1982) in *Superoxide Dismutase* (Oberley, L. W., ed) Vol. II, pp. 15–30, CRC Press, Boca Raton, FL
36. Turrens, J. F., Alexandre, A., and Lehninger, A. L. (1985) *Arch. Biochem. Biophys.* **237,** 408–414
37. Nohl, H., and Jordan, W. (1986) *Biochem. Biophys. Res. Commun.* **138,** 533–539
38. Voet, D., Voet, J. G., and Pratt, C. W. (1999) *Fundamentals of Biochemistry*, John Wiley & Sons, Inc., New York
39. Halliwell, B., and Gutteridge, J. M. C. (1989) *Free Radicals in Biology and Medicine*, Oxford University Press Inc., New York